IBRO Neuroscience Reports 12 (2022) 366–376

Contents lists available at ScienceDirect

IBRO Neuroscience Reports

journal homepage: www.sciencedirect.com/journal/IBRO-Neuroscience-Reports

Research paper

Early mobilization in spinal cord injury promotes changes in microglial dynamics and recovery of motor function

Kohta Asano [a,b,*], Takeshi Nakamura [a], Kengo Funakoshi [b]

[a] Rehabilitation Science, Yokohama City University School of Medicine, 3-9 Fukuura, Kanazawa-ku, Yokohama, Kanagawa 236-0004, Japan
[b] Neuroanatomy Yokohama City University School of Medicine, 3-9 Fukuura, Kanazawa-ku, Yokohama, Kanagawa 236-0004, Japan

ARTICLE INFO

Keywords:
Spinal cord injury
Early mobilization
Microglia
Neuroinflammation
Matrix metalloproteinases
Motor function

ABSTRACT

In the acute phase of spinal cord injury, the initial injury triggers secondary damage due to neuroinflammation, leading to the formation of cavities and glial scars that impair nerve regeneration. Following injuries to the central nervous system, early mobilization promotes the recovery of physical function. Therefore, in the present study, we investigated the effects of early mobilization on motor function recovery and neuroinflammation in rats. Early mobilization of rats with complete spinal cord transection resulted in good recovery of hindlimb motor function after 3 weeks. At 1 week after spinal cord injury, the early-mobilized rats expressed fewer inflammatory M1 microglia/macrophages and more anti-inflammatory M2 microglia. In addition, significantly more matrix metalloproteinase 2 (MMP2)-positive cells were observed at the lesion site 1 week after injury in the early-mobilized rats. Multiple labeling studies suggested that many MMP2-positive cells were M2 microglia. MMP9-positive cells that highly co-expressed GFAP were also observed more frequently in the early-mobilized rats. The density of growth-associated protein-positive structures in the lesion center was significantly higher in the early-mobilized rats at 3 weeks after spinal cord injury. The present results suggest that early mobilization after spinal cord injury reduced the production of M1 microglia/macrophages while increasing the production of M2 microglia at the lesion site. Early mobilization might also activate the expression of MMP2 in M2 microglia and MMP9 in astrocytes. These cellular dynamics might suppress neuroinflammation at the lesion site, thereby inhibiting the progression of tissue destruction and promoting nerve regeneration to recover motor function.

1. Introduction

Disorders of the central nervous system (CNS) can cause motor and sensory impairments that significantly disrupt daily life. Voluntary motor dysfunction may lead to gait disturbances and limited range of motion in several joints, whereas sensory impairments can lead to skin ulcers and dysuria, with competition by autonomic nervous system disorders such as smooth muscle dysfunction and neuropathic pain. Disorders of the CNS are thus a major therapeutic target of rehabilitation and neurological physical therapy.

Although several new treatments have been developed for spinal cord injury (SCI) (Venkatesh, et al., 2019), rehabilitation remains a major component of SCI treatment. Rehabilitation for SCI has 2 main objectives. The first objective is to improve unimpaired physical function and maintain muscle strength for voluntary movement as much as possible. Maintaining muscle strength leads to increased independence and activity in daily life. The second objective is to prevent secondary complications, such as pressure ulcers and urinary tract infection, which can lead to septic shock and joint contractures that interfere with daily life. Rehabilitation approaches play an important role in maintaining a healthy life for SCI patients, but their effectiveness for severe sensory impairment and motor paralysis is limited. One reason for this is that most patients with SCI in the acute phase require rest and are not able to undergo rehabilitation. The priority in the acute phase is to stabilize the

Abbreviations: CNS, central nervous system; SCI, spinal cord injury; CSPGs, chondroitin sulfate proteoglycans; MMPs, matrix metalloproteinases; IL1β, interleukin-1β; TNF-α, tumor necrosis factor-α; EM, early mobilization; NEM, non-early mobilization; BBB score, The Basso, Beattie, Bresnahan locomotor rating scale score; PBS, phosphate-buffered saline; PFA, paraformaldehyde; PBST, PBS containing 0.05% Tween 20; iNOS, inducible nitric oxide synthase; tomato lectin, *Lycopersicon Esculentum* lectin; DAPI, 4′,6-diamidino-2-phenylindole; GFAP, glial fibrillary acidic protein; GAP43, growth associated protein 43.

* Corresponding author at: Rehabilitation Science, Yokohama City University School of Medicine, 3-9 Fukuura, Kanazawa-ku, Yokohama, Kanagawa 236-0004, Japan.
E-mail address: uncleka@yokohama-cu.ac.jp (K. Asano).

https://doi.org/10.1016/j.ibneur.2022.04.002
Received 11 October 2021; Received in revised form 11 April 2022; Accepted 11 April 2022
Available online 14 April 2022

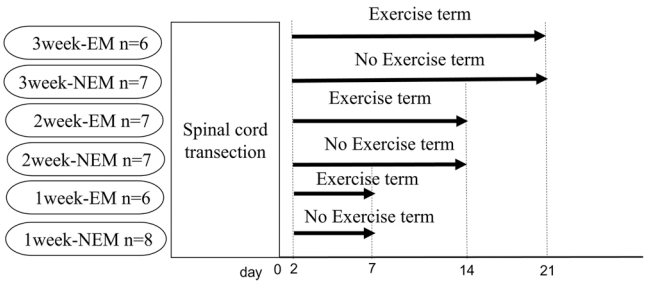

Fig. 1. Schematic diagram of the experiments.

vertebrae after spinal fusion surgery and to control blood circulation during spinal shock. We speculated that this limitation is a major factor delaying the recovery of physical functions in SCI patients.

A previous study reported that early mobilization promotes the recovery of physical function and quality of life in patients with stroke (The AVERT Trial Collaboration group). We hypothesized that early mobilization may also be effective for promoting the recovery of motor function after SCI. While Brown et al. (2011) demonstrated that very early exercise improves recovery of motor function in rats with SCI, the mechanisms underlying the recovery of motor function remain unclear because they did not perform complete histological assessment. In the present study, therefore, we applied early exercise therapy to rats with SCI and evaluated the recovery of motor function and histological changes at the lesion site in the spinal cord.

Neuroinflammation after SCI is induced by secondary damage following the initial injury, and involves edema, hemorrhage, ischemia, infiltration of inflammatory cells, release of cytotoxic factors, and cell death. In the acute phase of neuroinflammation, the blood-brain barrier and blood-spinal cord barrier are infiltrated by proinflammatory M1 microglia/macrophages at the site of the SCI, where they secrete several inflammatory cytokines and factors such as interleukin-1β (IL1β), tumor necrosis factor-α (TNFα), and matrix metalloproteinases (MMPs). Neuroinflammation also leads to the proliferation of astrocytes and microglia, and enhances the production of chondroitin sulfate proteoglycans (CSPGs), an extracellular matrix component that inhibits axon regeneration. CSPGs and inflammatory cytokines secreted by activated astrocytes and microglia promote the formation of glial scars (Adams and Gallo, 2018; Dyck and Karimi-Abdolrezaee, 2015; Rolls, et al., 2008).

Activation of M2 microglia/macrophages following the activation of M1 microglia/macrophages leads to neuroprotective and anti-inflammatory effects. Production of anti-inflammatory cytokines and factors such as interleukin-10 and enzymes such as arginase-1, MMP9, and MMP2 is suggested to promote nerve repair and regeneration (Ledeboer et al., 2000). MMP9 and MMP2 are involved in acute and subacute wound healing and glial scar formation after SCI (Hsu et, al. 2008). Interactions between microglial activation and MMP production were recently suggested to suppress neuroinflammation (Bellver-Landete et al., 2019; Cunha, et al., 2016). Interestingly, early increases and maintenance of M2 microglia induced by exercise therapy has been reported in obese rats (Jeong, et al., 2015).

Previous animal studies showed that exercise therapy significantly reduces the expression of the pro-inflammatory cytokines TNFα and IL1β in the spinal cord in rats with contusion SCI (Dugan et al., 2020). In patients with chronic SCI, exercise also reduces serum levels of systemic inflammatory markers (Neefkes-Zonneveld et al., 2015). The involvement of macrophages/microglia in the suppression of inflammation induced by early exercise, however, has not yet been investigated, although early exercise does appear to change the responses of macrophages/microglia in rats with SCI (Chhaya et al., 2019). We hypothesized, therefore, that exercise therapy introduced during the acute phase of SCI in rats might suppress neuroinflammation and promote functional motor recovery by activating M2 macrophages/microglia, which have anti-inflammatory effects in association with MMP2/MMP9 dynamics.

In this study, we performed a complete transection of the thoracic spinal cord to evaluate whether axonal regeneration contibutes to the recovery of motor function. As a model for inflammation, the transection injury is used less frequently than contusion injury, because the inflammation might be limited due to the small extent of the primary damage (Sharif-Alhoseini et al., 2017). On the other hand, complete spinal cord transection is a useful model for evaluating the relationship between regenerated axons beyond the lesion site and the recovery of motor function because sprouting of intact axons passing through the lesion site might be involved in the recovery of motor function in the other SCI models such as contusion and hemisection.

2. Material and methods

Wistar female rats (SLC, Hamamatsu, Japan, n = 41) were randomly assigned to early mobilization (EM) or non-early mobilization (NEM) groups. Survival periods for the EM and NEM groups were 1 week (EM; n = 6, NEM; n = 8), 2 weeks (EM; n = 7, NEM; n = 7), or 3 weeks (EM; n = 6, NEM; n = 7) (Fig. 1).

Experiments were performed when the rats were 9–12 weeks old and weighed 130–150 g. They were housed in acrylic boxes, 2 or 3 at a time, in a temperature-controlled environment with a 12-h day/night cycle. Food and water were available ad libitum. Every effort was made to minimize animal suffering and to reduce the number of animals used. Animals that exhibited severe respiratory depression or could not drink water independently were killed humanely by an overdose of isoflurane anesthesia. The animal experimental designs were approved by the Institutional Animal Care and Use Committee of Animal Research Center, Yokohama City University Graduate School of Medicine.

2.1. Spinal cord transection operation procedures: posterior approach to the thoracic spine

All rats were operated on under inhalation anesthesia with isoflurane (concentration: 2%). The rats were placed prone on the operating table, and the surgical field was cleared by shaving the dorsal body hair as closely as possible with electric clippers. The bilateral subscapularis angle and the spinous process of the L1 vertebra were identified, and a mark was made above each spinous process from T6 to the L1 vertebra. After disinfecting the surgical field with povidone-iodine solution (10% solution, Kaneichi Pharmaceuticals, Osaka, Japan), a 1.2-inch incision was made in the midline to expose the skin along the marked points, and a deep median dissection was performed through the superficial thoracodorsal fascia. The erector spinae muscles were shallowly dissected bilaterally, and an animal wound retractor was applied. The isoflurane concentration was then lowered to 1.5% to reduce hypoxia-induced brain damage, and the Th9, Th10, and Th11 erector spinae were completely dissected from both sides, and both spinous processes were peeled off with a scalpel (No. 15 Feather surgical blade, Feather Inc., Osaka, Japan). The spinous processes of Th9 and Th10 were folded with tweezers to expose the Th10 lamina of the vertebral arch without the erector spinae, and a laminectomy was performed to totally expose the dorsal spinal cord. Bone fragments were removed as much as possible, and the spinal cord at the T10 level was cut in an arc from the back (right side of the rat) to the front (left side of the rat) with a sharp scalpel (same as No. 11) to confirm that the transection of spinal cord was complete in both the rostral and caudal directions (Lu et al., 2012). After complete hemostasis was achieved, the muscle was sutured in 2 layers and the skin wound was closed with 6–7 sutures using a 3–0 mm nylon filament. To properly evaluate the effects of SCI on neuroinflammation, no antibiotics, analgesics, or anti-inflammatory drugs were administered.

2.2. Postoperative management

After the surgery, the rats were covered with bedding material in an acrylic cage to maintain their body temperature until they awoke.

Fig. 2. Early mobilization in the EM group. The rat moves forward and backward on the wire mesh using only the forelimbs (arrows), while the hip joint is manually manipulated to keep the rat moving.

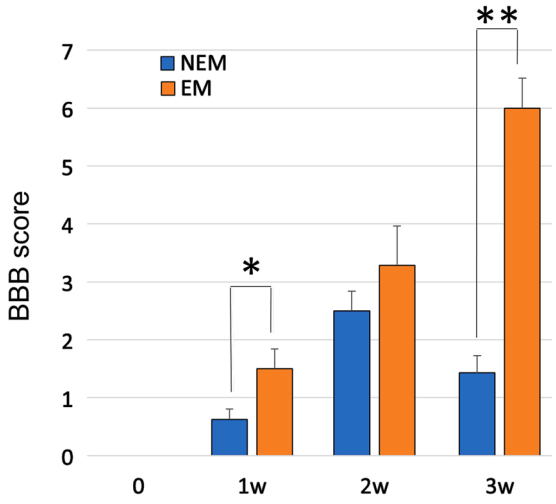

Fig. 3. BBB scores of the NEM and EM groups were compared at 1, 2, and 3 weeks after injury. Early mobilization significantly improved hindlimb motor function at 1 and 3 weeks after injury. Data are presented as mean ± SEM. * p-value = 0.026, * * $p < 0.005$.

Urination was achieved in the usual way. From the postoperative period until the endpoint, the bladder was emptied by the Credé maneuver 2–3 times a day to prevent urinary tract infection and bladder injury causing bladder spasm.

2.3. Early mobilization

Early mobilization was started within 48 h after surgery and performed 5 days a week for 10 min each time. Before early mobilization, the bladders of the rats were emptied by the Credé maneuver, and after the early mobilization training, the open field apparatus in the laboratory (20" [51 cm] wide x 40" [102 cm] high x 4" [10 cm] deep) was cleaned and disinfected with 70% ethanol. In the forced forelimb training exercise, the rat was placed with its forelimbs on a metal wire mesh that was easy to grasp, and allowed to move forward and backward on the wire mesh using only the forelimbs. The examiner elevated the hind limbs off the grid while stabilizing the rat's pelvis with the index finger of the right hand and holding the femurs with the left hand to support the hip joints, adjusting the direction to keep the rat moving. All treatments were performed by the same examiner (Fig. 2).

2.4. Behavioral observation and evaluation

The Basso, Beattie, Bresnahan (BBB) locomotor rating scale was used to assess hindlimb motor function. All rats in all groups were assessed for forward running by a skilled examiner to see what motor patterns emerged over a 5-min period (Basso et al. 1995). Because the motor patterns of the limbs are easily altered by urination and defecation, it was necessary to empty the bladder by performing the Credé maneuver before evaluating the motor function of the hindlimbs.

2.5. Immunohistochemical examination

2.5.1. Tissue preparation

After behavioral assessment during the survival period, rats in the 1-week EM group (n = 6), 1-week NEM group (n = 8), 3-week EM group (n = 6), and 3-week NEM group (n = 7) were anesthetized with 5% isoflurane to a surgical plane of anesthesia and transcardially perfused with 0.9% saline (500 units of heparin/ml) from the ascending aorta to remove blood, followed by 25 mM phosphate-buffered saline (PBS, pH 7.4) containing 4% paraformaldehyde (PFA). The cervical to sacral spinal cord was dissected out along with the vertebrae between Th7 and Th12, as the central part of the injury is more vulnerable. The spinal cords were post-fixed in 4% PFA for 24 h and then placed in 25 mM PBS containing 30% sucrose for at least 2 days. The spinal cord specimens were carefully separated from the accompanying vertebral bodies and arches under a stereomicroscope. After exclusion of severely damaged cords, the thoracic spinal cords including the lesion site of the 1-week EM (n = 4), 1-week NEM (n = 4), 3-week EM (n = 4), and 3-week NEM (n = 4) were placed in tissue freezing medium (General Data Company Inc., Cincinnati, OH, USA). Frozen thoracic spinal cords were serially sectioned into 12-μm-thick horizontal sections using a cryostat (CM3050 S, Leica, Nussloch, Germany), and thaw-mounted on gelatin-coated slides. A total of 6–8 sections were arranged on 8 sets of gelatin-coated slides. All sections were dried at room temperature for 1 h and stored at − 60 °C until immunostaining.

2.5.2. Immunohistochemistry staining

The sections were fixed in 0.1 M phosphate-buffered PBS containing 4% PFA for 30 min. They were washed in 0.025 M PBS 3 times for 5 min each, and in 0.025 M PBS containing 0.05% Tween 20 (PBST, pH 7.4) for 30 min. After applying 20-fold diluted blocking reagent (Megmilk Snow Brand Co. Ltd., Tokyo, Japan) for 1 h, a series of sections was incubated overnight at 4 °C in a moist chamber with a mixture of primary antibodies (described below), diluted in 1% normal donkey serum, 0.2% bovine serum albumin, and 0.1% NaN_3 in 0.025 M PBST. After washing once with 0.025 M PBST and twice with 0.025 M PBS, the completely light-shielded sections were incubated with a mixture of secondary antibodies (indicated below) for 90 min at room temperature.

2.5.3. Primary and secondary antibodies

2.5.3.1. Evaluation in the acute phase. Spinal cord sections of 1-week EM rats and 1-week NEM rats were used to evaluate the effects of early mobilization on microglia/macrophages dynamics and MMP expression in the acute phase.

2.5.3.1.1. M1 and M2 microglia/macrophages. Mouse monoclonal antibodies against CD163 (1:100; MCA342R, Bio-Rad, Hercules, CA, USA) and rabbit polyclonal antibodies against inducible nitric oxide synthase (iNOS; 1:100; ab15323, Abcam, Cambridge, UK) were used as primary antibodies to label M2 microglia/macrophages and M1 microglia/macrophages, respectively. Cy3-conjugated anti-mouse IgG (10 μg/ml; Jackson ImmunoResearch Laboratories, West Grove, PA, USA) and Cy5-conjugated anti-rabbit IgG (10 μg/ml; Jackson ImmunoResearch Laboratories) were used as secondary antibodies, and DyLight 488-conjugated *Lycopersicon Esculentum* (Tomato) lectin (Vector Laboratories,

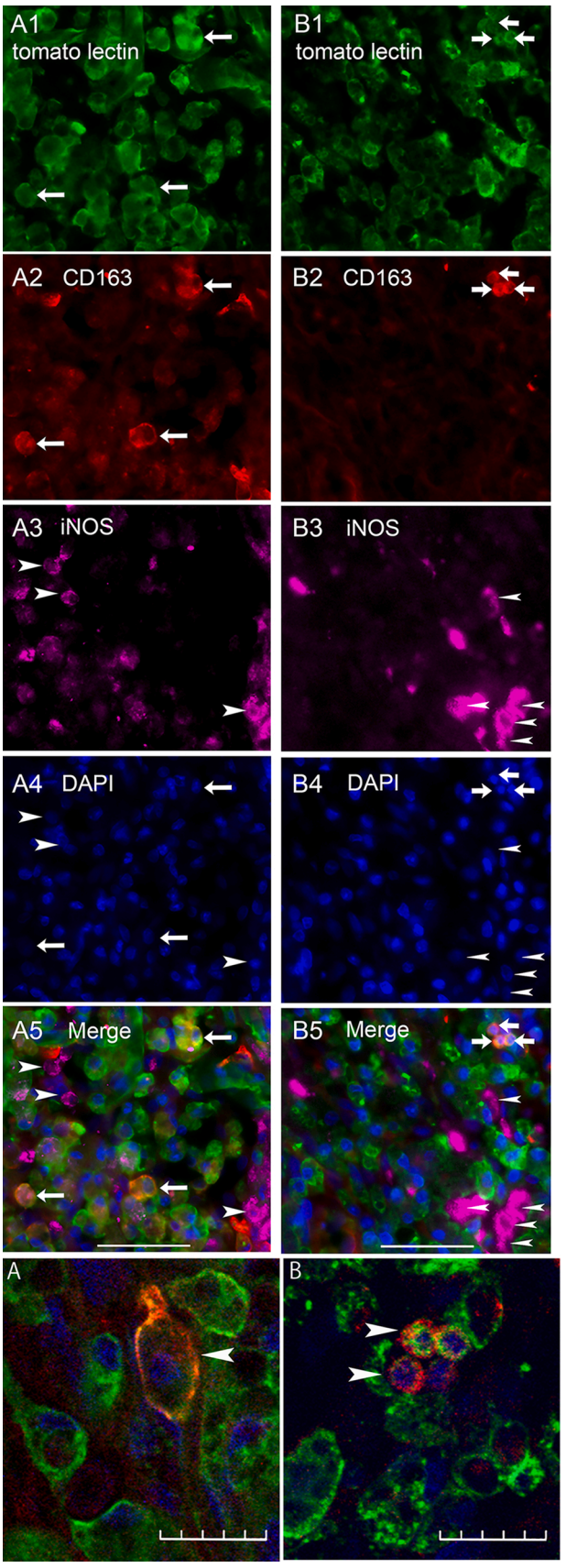

(caption on next column)

Fig. 4. Fig. 4-1. Images of quadruple staining with tomato lectin (green; **A1** and **B1**), CD163 (red; **A2** and **B2**), iNOS (violet; **A3** and **B3**), and DAPI (blue; **A4** and **B4**), as well as merged images (**A5** and **B5**) at the lesion site. Images of the 1-week (1w) EM group are shown in the left row (**A1**-**5**), and those of the 1-week NEM group are shown in the right row (**B**1-**5**). Arrows indicate cells positive for both CD163 and tomato lectin. Arrowheads indicate iNOS-positive cells. Scale bars: 50 μm. Fig.4-2. A**, B**: Merged confocal images of triple staining with tomato lectin, CD163, and DAPI (enlarged images of Fig. 4–1 A***5 and B5***). Arrowheads indicate cells positive for both CD163 and tomato lectin. Scale bars: 20 μm.,.

Burlingame, CA, USA) was used with 4′,6-diamidino-2-phenylindole (DAPI) to label microglia.

2.5.3.1.2. Activated astrocytes/MMP9. Goat polyclonal antibodies against glial fibrillary acidic protein (GFAP; 1:100; ab53554, Abcam) and rabbit polyclonal antibodies against MMP9 (1:100; 10375–2-AP; Proteintech, Rosemont, IL, USA) were used as primary antibodies to label astrocytes and MMP9-positive structures, respectively. Alexa Fluor 647-conjugated donkey anti goat IgG (10 μg/ml; Jackson ImmunoResearch Laboratories) and Alexa Fluor 488-conjugated donkey anti rabbit IgG (10 μg/ml; Jackson ImmunoResearch Laboratories) were used as secondary antibodies with DAPI.

2.5.3.1.3. Axon regression/MMP2/resident microglia. Mouse monoclonal antibodies against growth associated protein-43 (GAP43; 1:500; ab12990, Abcam) and rabbit polyclonal antibodies against MMP2 (1:200; 10373–2-AP, Proteintech) were used as primary antibodies to label growth cones and MMP2-positive structures, respectively. Cy5-conjugated anti-mouse IgG (10 μg/ml; Jackson ImmunoResearch Laboratories) and Cy3-conjugated anti-rabbit IgG (10 μg/ml; Jackson ImmunoResearch Laboratories) were used as secondary antibodies, and DyLight 488-conjugated tomato lectin (Vector Laboratories) was used with DAPI to label microglia.

2.5.3.2. Evaluation in the subacute phase. Spinal cord sections of 3-week EM rats and 3-week NEM rats were used to evaluate the effects of early mobilization on the histology of the lesion site in the subacute phase.

2.5.3.2.1. Histochemical analysis of the lesion site. Goat polyclonal antibodies against glial fibrillary acidic protein (GFAP; 1:100; ab53554, Abcam) and rabbit polyclonal antibodies against fibronectin (1:100; PAA037Ga01, Cloud-Clone Corp.) were used as primary antibodies to label astrocytes and fibronectin-positive structures, respectively. Alexa Fluor 488-conjugated donkey anti rabbit IgG (10 μg/ml; Jackson ImmunoResearch Laboratories) and Cy3-conjugated donkey anti rabbit IgG (10 μg/ml; Jackson ImmunoResearch Laboratories) were used as secondary antibodies, and DyLight 488-conjugated tomato lectin (Vector Laboratories) was used with DAPI to label microglia.

2.5.3.2.2. GAP43/collagenⅣ/GFAP. Mouse monoclonal antibodies against GAP43 (1:500; ab12990, Abcam), rabbit polyclonal antibodies against collagenⅣ (1:100; ab6586, Abcam), and goat polyclonal antibodies against glial fibrillary acidic protein (GFAP; 1:100; ab53554, Abcam) were used as primary antibodies to label growth cones, collagen fibers, and astrocytes, respectively. Cy5-conjugated anti-mouse IgG (10 μg/ml; Jackson ImmunoResearch Laboratories), Cy3-conjugated donkey anti rabbit IgG (10 μg/ml; Jackson ImmunoResearch Laboratories), and Alexa Fluor 488-conjugated donkey anti goat IgG (10 μg/ml; Jackson ImmunoResearch Laboratories) were used as secondary antibodies with DAPI.

2.5.3.2.3. Axon regression/MMP2/resident microglia. Mouse monoclonal antibodies against GAP43 (1:500; ab12990, Abcam) and rabbit polyclonal antibodies against MMP2 (1:200; 10373–2-AP, Proteintech) were used as primary antibodies to label growth cones and MMP2-positive structures, respectively. Cy5-conjugated anti-mouse IgG (10 μg/ml; Jackson ImmunoResearch Laboratories) and Cy3-conjugated anti-rabbit IgG (10 μg/ml; Jackson ImmunoResearch Laboratories) were used as secondary antibodies, and DyLight 488-conjugated tomato lectin (Vector Laboratories) was used with DAPI to label microglia.

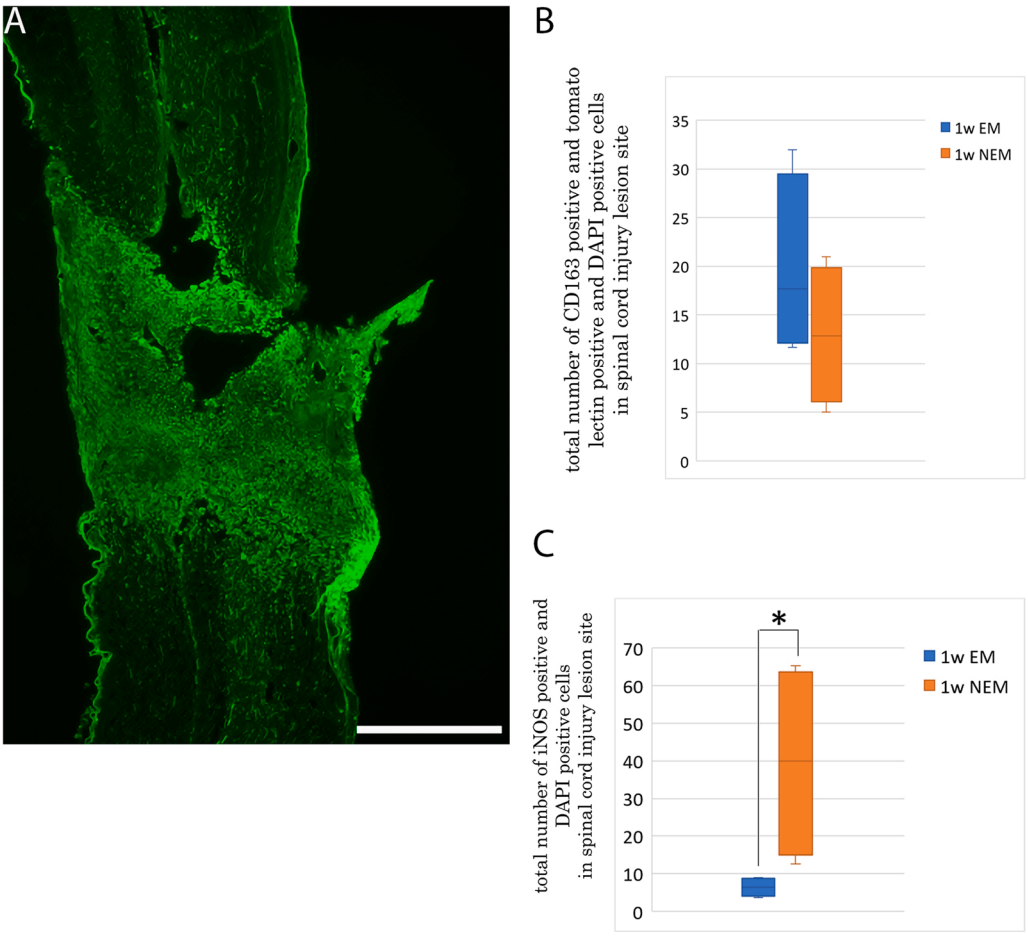

Fig. 5. A: Overview of the spinal cord in the 1-week EM group. Tomato lectin-positive cells accumulated in the lesion center but are also observed in the surrounding area. Scale bar: 500 μm. B: Comparison of the number of cells positive for CD163 and tomato lectin at the lesion site including the surrounding area between the 1-week NEM and 1-week EM groups. Data are presented as mean ± SEM. No significant difference was detected between the 2 groups. C: Comparison of the number of iNOS-positive cells at the lesion site between the 1-week NEM and 1-week EM groups. Data are presented as mean ± SEM. * p-value= 0.029.

2.5.3.3. Cell counts and imaging. An average of 3 sections per slide of 1-week EM (n = 4) and 1-week NEM (n = 4), and 3-week EM (n=4) and 3-week NEM (n=4) was analyzed. All stained sections were observed with a scanning all-in-one fluorescence microscope (BZ-x810, Keyence Inc., Osaka, Japan). CD163-positive, iNOS-positive, MMP2-positive and MMP9-positive cells expressed in lesion site including the surrounding area were counted at 40x using the analyzer application. Triple immunofluorescence images of CD163/ tomato lectin/ DAPI, and MMP2/ tomato lectin/ DAPI were also acquired with a confocal laser scanning microscope (Olympus Fluo View FV1000, Tokyo, Japan) at 60x.

2.5.3.4. Void/ cavity measurement. An average of 3 sections per slide of 3-week EM (n = 4) and 3-week NEM (n = 4) was analyzed. All stained sections were observed with a scanning all-in-one fluorescence microscope (BZ-x810, Keyence Inc.). The area of the voids or cavities was measured at 10x using an analyzer application (BZ-X Analyzer, Keyence Inc.).

2.5.3.5. GAP43 structure measurement. An average of 3 sections per slide of 3-week EM (n = 3) and 3-week NEM (n = 3) was analyzed. All stained sections were observed with a scanning all- in-one fluorescence microscope (BZ-x810, Keyence Inc.). The lesion center was defined as a zone negative for GFAP. The areas of the lesion center and GAP43-positive structures were measured at 20x using an analyzer application (BZ-X Analyzer, Keyence Inc.).

2.6. Data analysis

Data collection and analysis were partially blinded. All data are expressed as mean ± standard error. BBB scores at each endpoint of EM and NEM were compared using Welch's t-test. The number of cells expressing CD163 and iNOS was compared between the 1-week EM and 1-week NEM groups using the Mann-Whitney U test. The numbers of cells expressing MMP2 and MMP9 were compared between the 1-week EM and 1-week NEM groups using the Mann-Whitney U test. The area of voids or cavities was compared between the 3-week EM and 3-week NEM groups using the Mann-Whitney U test. The areas of the lesion center and GAP43-positive structures were compared between 3-week EM and 3-week NEM groups using Welch's t-test. A p-value < 0.05 was considered statistically significant. The software SPSS Statistics 22.0 (Armonk, IBM Corporation, NY, USA) was used to analyze the data.

3. Results

3.1. Motor function recovery; open field test

Recovery of hindlimb motor function on the BBB rating scale differed markedly between groups with and without early mobilization for 3 weeks (Fig. 3). Although both groups were completely paralyzed on the day of spinal cord transection, the BBB score of the EM group gradually increased from the first week of injury (1.5 ± 0.34 at 1 week, 3.29 ± 0.68 at 2 weeks, and 6.0 ± 0.52 at 3 weeks), whereas the improvement in the BBB score of the NEM group was limited to only about 1–2 points (0.63 ± 0.18 at 1 week, 2.5 ± 0.34 at 2 weeks, and 1.43 ± 0.30 at 3 weeks). The BBB score significantly differed between the EM and NEM groups after 1 week (* $p = 0.026$) and 3 weeks (** $p < 0.005$). Each endpoint of the BBB score is shown in the Supplementary video data.

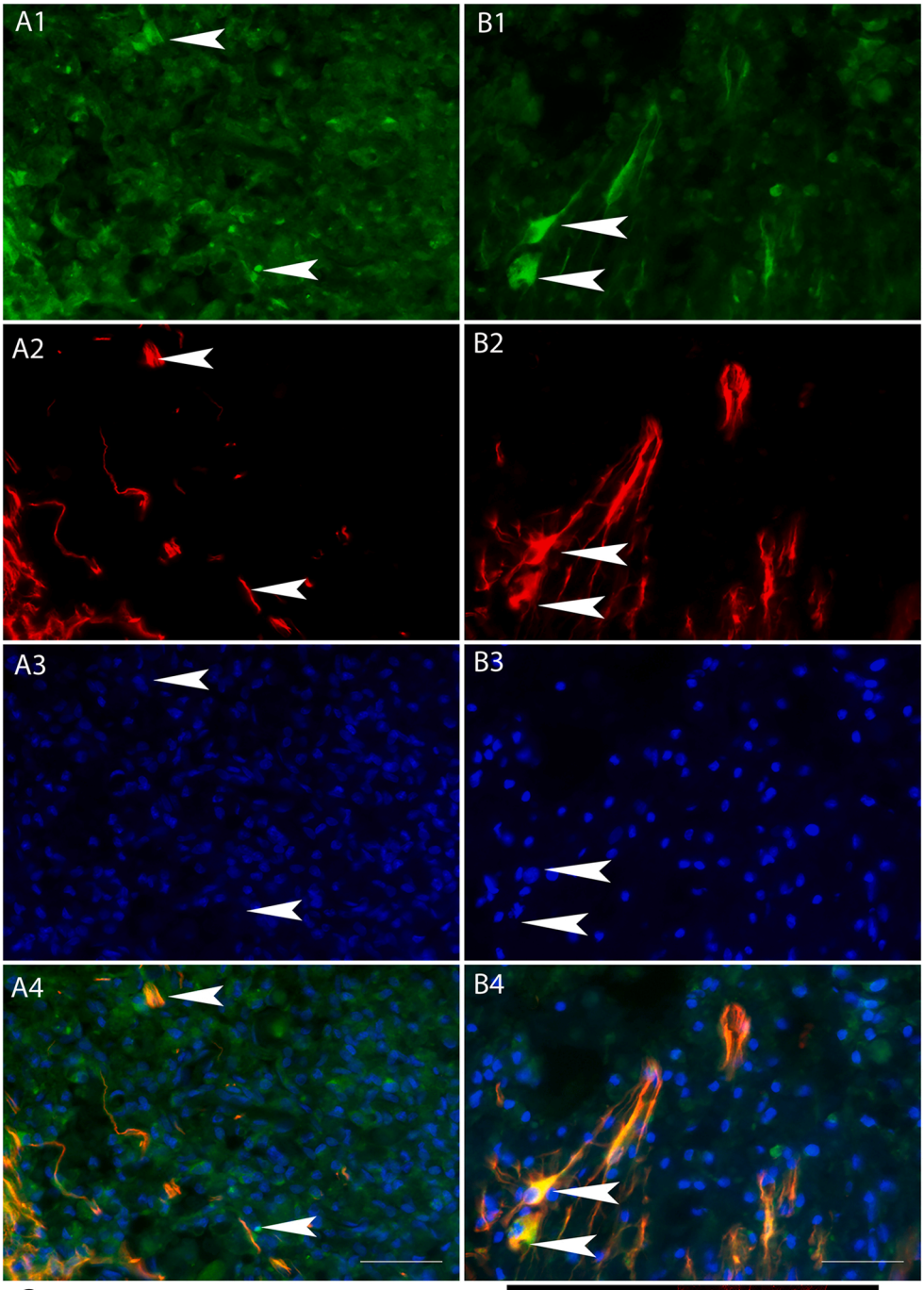

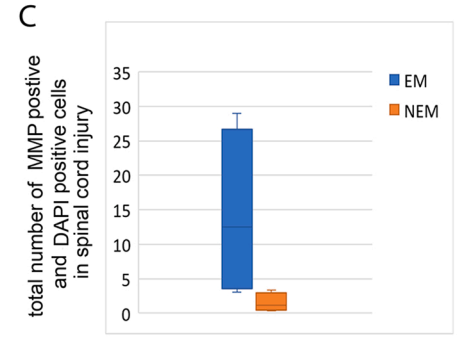

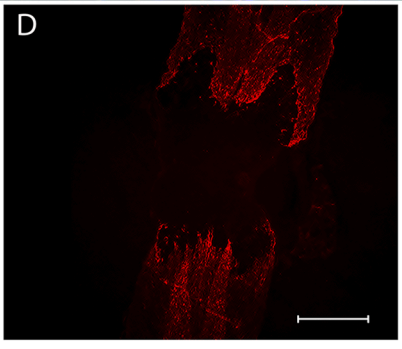

Fig. 6. A, B: Images of triple staining with MMP9 (green; **A1** and **B1**), GFAP (red; **A2** and **B2**), and DAPI (blue; **A3** and **B3**), as well as merged images (**A4** and **B4**) at the lesion site. Images of the 1-week EM group are shown in the right row (**A1-4**), and those of the 1-week NEM group are shown in the left row (**B1-4**). Arrowheads show cells positive for both MMP9 and GFAP. Scale bars: 50 μm. **C**: Comparison of the number of MMP9-positive cells at the lesion site including the surrounding area between the 1-week NEM and 1-week EM groups. Data are presented as mean ± SEM. No significant difference was detected between the 2 groups. **D**: Overview of the spinal cord in the 1-week NEM group. GFAP-positive fibers were observed in the surrounding area, but not at the lesion center. Scale bar: 500 μm.

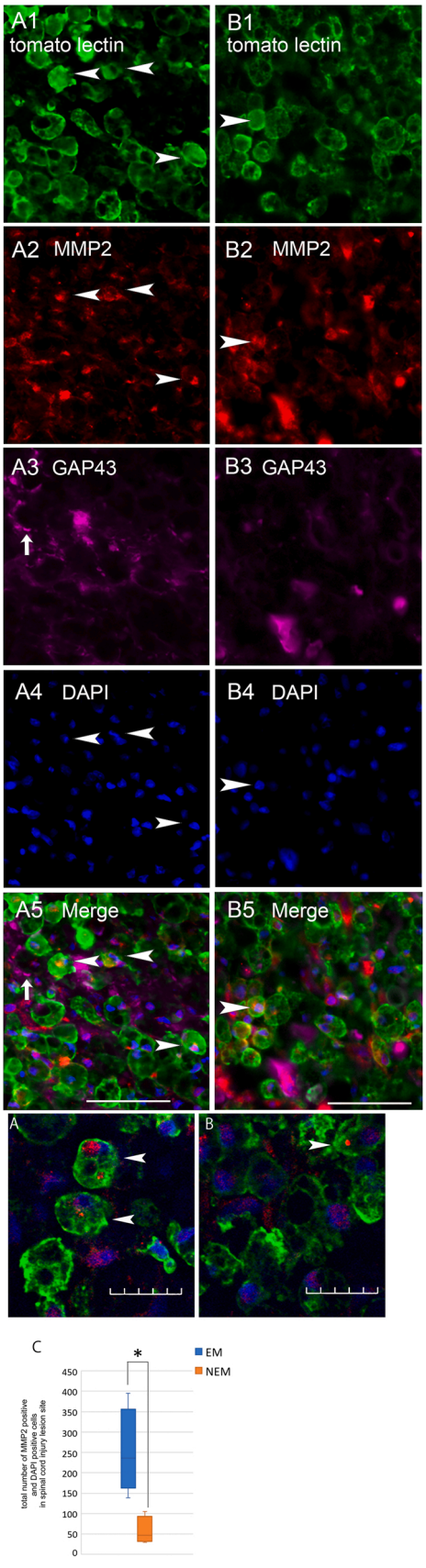

(caption on next column)

Fig. 7. Fig. 7-1. A, B: Images of quadruple staining with tomato lectin (green; **A1** and **B1**), MMP2 (red; **A2** and **B2**), GAP43 (violet; **A3** and **B3**), and DAPI (blue; **A4** and **B4**), as well as merged images (**A5** and **B5**) at the lesion site. Images of 1-week EM group are shown in the left row (**A1**-**5**), and those of the 1-week NEM group are shown in the right row (**B1**-**5**). Arrowheads indicate cells positive for both tomato lectin and MMP2. Arrows indicate GAP43-positive structures. Scale bars: 50 μm. Fig.7-2. **A, B**: Merged confocal images of triple staining with tomato lectin, MMP2, and DAPI (enlarged images of Fig. 7–1 A5 and B5). Arrowheads indicate cells positive for both MMP2 and tomato lectin. Scale bars: 20 μm. **C**: Comparison of the number of MMP2-positive cells at the lesion site including the surrounding area between the 1-week NEM and 1-week EM groups. Data are presented as mean ± SEM. * p-value = 0.029.

3.2. *Immunohistochemical analysis in the acute phase*

3.2.1. *CD163/ iNOS/ tomato lectin/ DAPI*

Quadruple staining for tomato lectin, CD 163, iNOS, and DAPI was performed (Fig. 4–1). Many cells in the lesion site were positive for tomato lectin and DAPI (Fig. 4–1 A, B). Tomato lectin- and DAPI-positive cells were resident microglia. Many CD163-positive cells were also positive for tomato lectin and DAPI with confocal microscopic observation (Fig. 4–2 A, B). These triple-positive cells were considered to be M2 microglia.

Many cells were positive for iNOS and DAPI. Few of these cells, however, were positive for tomato lectin (Fig. 4–1 A, B). Therefore, we considered the iNOS-positive and DAPI-positive cells to be M1 microglia/macrophages.

The number of cells positive for CD163 and tomato lectin at the lesion site tended to be higher in the 1-week EM group (19.75 ± 4.67) than in the 1-week NEM group (12.92 ± 3.57), although no significant difference was observed between the 2 groups. The number of iNOS-positive cells at the lesion site was significantly lower in the 1-week EM group (6.42 ± 1.25) than in the 1-week NEM group (39.5 ± 13.1). (Fig. 5B, C).

3.2.2. *MMP9/ GFAP/ DAPI*

Triple staining for MMP9, GFAP, and DAPI was performed (Fig. 6). MMP9-positive cells were observed in the surrounding areas, where some MMP9-positive cells were also positive for GFAP, whereas few MMP9-positive cells were present in the lesion center. The number of MMP9 positive cells in the lesion sites tended to be higher in the 1-week EM group (14.25 ± 6.14) than in the 1-week NEM group (1.5 ± 0.67), although the difference between the 2 groups was not significant.

3.2.3. *MMP2/ GAP43/ tomato lectin/ DAPI*

Quadruple staining for tomato lectin, MMP2, GAP43, and DAPI was performed (Fig. 7–1). The number of MMP2-positive cells was significantly higher in the 1-week EM group (251.5 ± 53.05) than in the 1-week NEM group (57.25 ± 16.89). Most of MMP2-positive cells were also positive for tomato lectin with confocal microscopic observation (Fig. 7–2 A, B).

In both 1-week EM and NEM groups, GAP43-positive structures were observed in rostral and caudal regions of the lesion site but not passing through the lesion site, and less frequently in the lesion center.

3.3. *Immunohistochemical analysis in the subacute phase*

3.3.1. *Tomato lectin/ GFAP/ fibronectin/ DAPI*

Quadruple staining for tomato lectin, GFAP, fibronectin, and DAPI was performed (Fig. 8). In the 3-week EM and NEM groups, a fibrous scar formed in the lesion center that was surrounded by glial tissue strongly positive for GFAP. Large voids or cavities were observed mainly in the surrounding area, but small voids were observed in the lesion center (Fig. 8). Many fibronectin-positive cells were observed in the surrounding area, but not in the lesion center. Tomato lectin-positive microglia were also observed in the surrounding area adjacent to

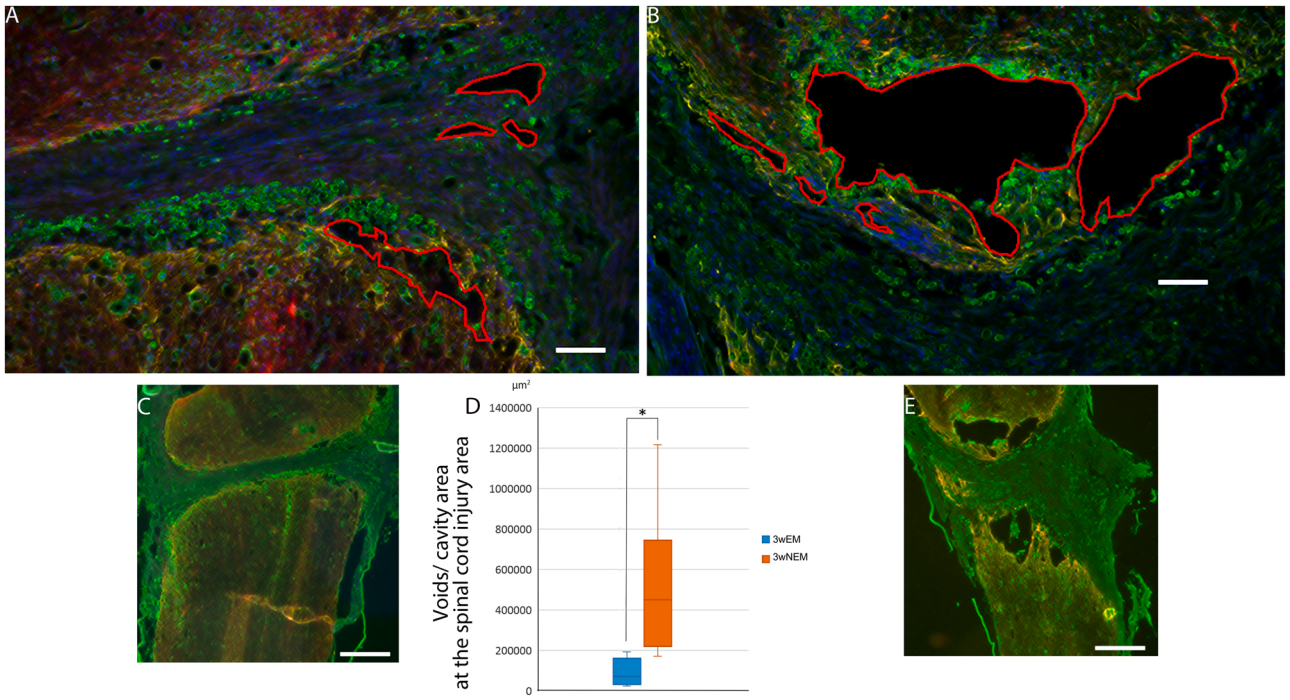

Fig. 8. A, B: Merged Images of quadruple staining with tomato lectin (green), GFAP (yellow), fibronectin (red), and DAPI (blue) at the spinal cord injury lesion. Image of the 3-week EM group is shown in **A** and that of the 3-week EM group is shown **B**. Red line enclosure indicates the void/cavity area. Scale bars: 100 μm. **C, E**: Overview of the spinal cord of the 3-week EM group (**C**) and the 3-week NEM group (**E**). Scale bars: 500 μm. **D**: Comparison of the void/cavity area at the spinal cord lesion sites between the 3-week NEM and 3-week EM groups. Data are presented as mean ± SEM. * p-value= 0.029.

some of the voids or cavities (Fig. 8A, B). The area of the voids or cavities was significantly smaller in the 3-week EM group (100735.7 ± 31951.6 μm^2) than in the 3-week NEM group (587473.0 ± 170683.5 μm^2).

3.3.2. *GAP43/ collagen/ GFAP*

Triple staining for GAP43, collagen, and GFAP was performed (Fig. 9). The area of GAP43- positive structures in the lesion center tended to be larger in the 3-week EM group (112542.9 ± 23355.7 μm^2) than in the 3-week NEM group (63738.6 ± 26833.3 μm^2), although the difference between the 2 groups was not significant. On the other hand, the area of the lesion center was significantly smaller in the 3-week EM group (577777. 0 ± 94213.9 μm^2) than in the 3-week NEM group (902203.4 ± 77381.1 μm^2). The density of GAP43-poisitive structures per lesion center, therefore, was significantly higher in the 3-week EM group (19.66 ± 4.02%) than in the 3-week NEM group (7.20 ± 3.46%).

3.3.3. *MMP2/ GAP43/ tomato lectin/ DAPI*

Quadruple staining for tomato lectin, MMP2, GAP43, and DAPI was performed (Fig. 10). In the 3-week EM groups, many GAP43-positive structures were observed in the area surrounding the lesion site where many tomato lectin-positive microglia were observed. Some GAP43 positive fibers ran through zones with no voids or cavities in the surrounding area (Fig. 10 A-5). In the 3-week NEM group, GAP43-positive fibers were also observed in the area surrounding the lesion site, but there was reduced space for the fibers to pass through due to the large cavities there (Fig. 9 B-5). GAP43-positive fibers passing though the fibrous lesion center were not observed in the 3-week EM and NEM groups.

4. Discussion

The present study showed that early mobilization was effective for the recovery of motor function. Previous studies reported that the effect of early mobilization on motor function recovery in rats with SCI is equivalent to that of anti-inflammatory drugs administered at the time of SCI (Alizadeh, et al. 2017; Zhang et al. 2019). Although the contusion injury model and complete transection model differ in many aspects, the findings of the present study demonstrated that early mobilization leads to the recovery of motor function after transection by regulating the immune response at the lesion site in the same way.

In the present study, we observed a trend toward a greater accumulation of cells positive for CD163 and tomato lectin at the lesion site in the EM group than in the NEM group at 1 week after injury. In addition, there were significantly fewer iNOS-positive cells at the lesion site in the EM group than in the NEM group at 1 week after injury. These observations suggest that early mobilization promoted the reduction of M1 microglia/macrophages and an increase in M2 microglia at the lesion site. In general, M1 microglia/macrophages are thought to promote neuroinflammation, while M2 microglia/macrophages suppress neuroinflammation. Therefore, early mobilization might contribute to the recovery of motor function by suppressing neuroinflammation in the injured tissues.

In SCI mice, MMP2 expressed at the lesion site is considered to be involved in the suppression of glial scar formation, degradation of fibrous scars, and removal of degenerated axons (Duchossoy, et al., 2001; Hsu, et al., 2006). In the present study, significantly more MMP2-positive cells were present at the lesion site at 1 week after injury in the EM group than in the NEM group. Early mobilization, therefore, might promote an increase in MMP2-positive cells at the lesion site. The finding that many of the MMP2-positive cells were also positive for tomato lectin suggests that MMP2 is expressed in microglia. Furthermore, tomato lectin-positive cells were frequently co-expressed with CD163, but not iNOS, suggesting that M2 microglia, but not M1 microglia/macrophages, express MMP2. The present results suggest that the increase in M2 microglia and decrease in M1 microglia/macrophages at the lesion site 1 week after injury correlated with the increase in MMP2, which might contribute to inhibit neuroinflammation and provide a favorable tissue environment for regenerating axons.

While the activity of MMP2, a subacute inflammatory mediator,

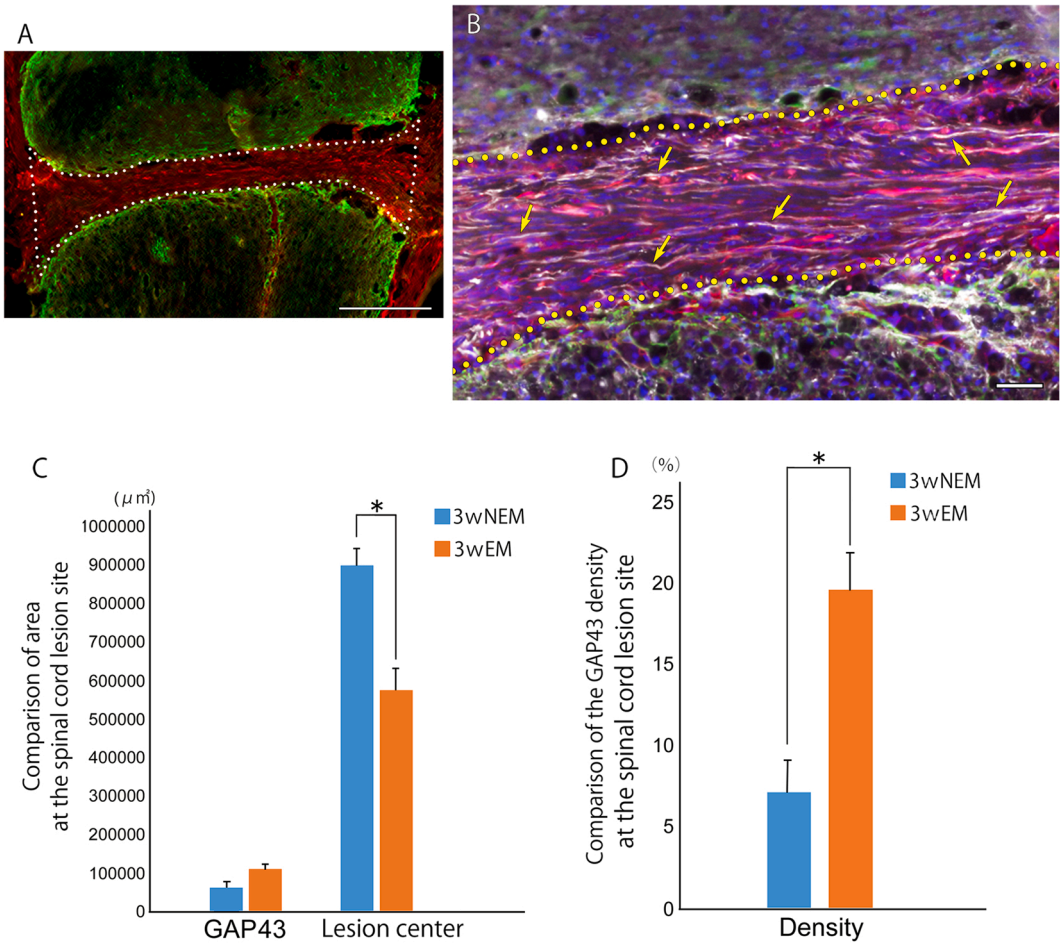

Fig. 9. A, B: Merged Images of quadruple staining with GFAP (green), GAP43 (white), and collagenIV (red) at the spinal cord injury lesion. Image of the 3-week EM group spinal cord lesion site overview is shown in **A.** Scale bar: 200 μm. The lesion center is enclosed by the white dotted line. **B:** Enlargement image of spinal cord lesion. Yellow arrows indicate representative GAP43 structures (white). The border of lesion center is indicated by the yellow dotted line. Scale bars: 50 μm. **C**: Comparison of the area of GAP43 structures and lesion center between the 3-week NEM and 3-week EM groups. Data are presented as mean ± SEM. * p-value= 0.011. **D**: Comparison of the GAP43 density of lesion center between the 3-week NEM and 3-week EM groups. Data are presented as mean ± SEM. * p-value= 0.016.

persists until 21 days after injury, the activity of MMP9 peaks at 1 day after injury and gradually declines within 14 days after injury, suggesting that MMP9 is an acute inflammatory mediator (Goussev, et al. 2003; Chiu, et al. 2018). In addition, in mice with SCI, MMP9 is upregulated in astrocytes and contributes to the formation of glial scars (Hsu et al., 2006, 2008; Trivedi et al., 2016, 2019). In the present study, MMP9-positive cells were mainly located in the surrounding area, where GFAP was frequently positive, suggesting that MMP9 is expressed in astrocytes and is involved in glial scar formation after SCI in rats. Furthermore, the finding that MMP9-positive cells tended to accumulate more in the EM group than in the NEM group might suggest that early mobilization promotes glial scar formation. As described before, however, early mobilization might also promote the accumulation of MMP2-positive cells at the lesion site. The effect of glial scar formation by MMP9, therefore, might have been attenuated by the activity of MMP2-positive cells, because MMP2 has inhibitory effects on glial scar formation.

In the present study, early mobilization resulted in the recovery of lower limb motor functions, but the mechanism is not clear. The presence of many GAP43-positive structures at the lesion site in the EM group suggests that regenerating axons frequently enter the lesion site in the subacute phase. The increase in M2 microglia accompanied by the upregulation of MMP2 at the lesion site 1 week after injury with early mobilization might have reduced neuroinflammation and increased the number of regenerating axons. In the EM group, furthermore, the areas of the lesion center and the voids/cavities were smaller at 3 weeks after injury, suggesting that the tissue damage was minimized. At the same time, many GAP43-positive structures passed through the intercellular spaces of microglia. M2 microglia are suggested to regulate the microenvironment at the site of injury and induce regenerating axons (Zhou et al. 2020). Therefore, M2 microglia-mediated repair of injured tissues might play an important role in the recovery of motor function promoted by early mobilization.

Although the present study did not provide the clear evidence of regenerating axons passing through the fibrous lesion center, it is possible that descending spinal projections such as the corticospinal tract regenerate beyond the lesion site to project to the lumbo-sacral spinal motor area within 3 weeks after SCI. A study in which treadmill training was combined with the administration of an enzyme that digests CSPGs, however, demonstrated that corticospinal tracts did not regenerate beyond the lesion area (Shinozaki, et al. 2016). On the other hand, another study demonstrated that treadmill training changes the plasticity of lumbar spinal neurons, particularly activating interneurons by increasing the peripheral sensory projections (Tillakaratne, et al. 2010). In sciatic nerve injury models, a significant increase in M1 microglia in the dorsal lumbar spinal cord leads to plastic changes in spinal cord neurons (Xu, et al. 2016; Nishihara, et al. 2020). Therefore, early mobilization might affect the dynamics of microglia and MMPs at the lumbar spinal cord level as well as at the lesion site, and thus might be involved in the recovery of hindlimb motor function.

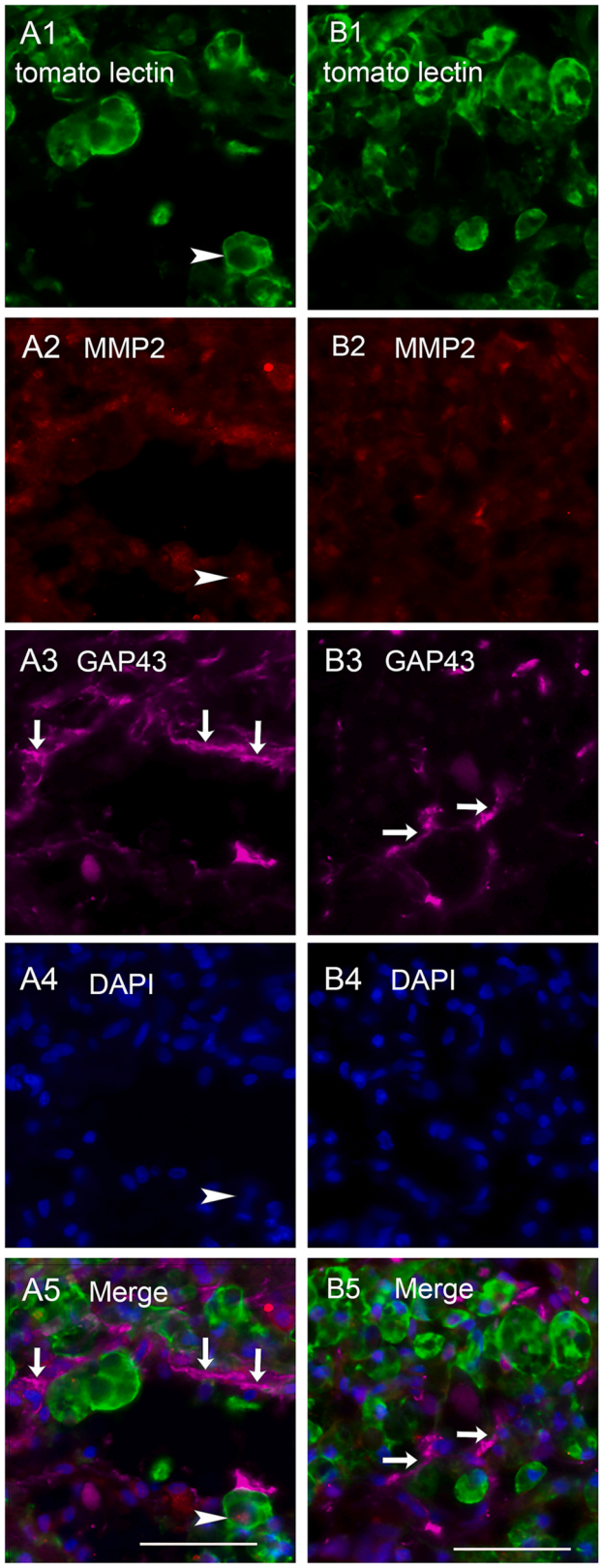

Fig. 10. **A**, **B**: Images of quadruple staining with tomato lectin (green; **A1** and **B1**), MMP2 (red; **A2** and **B2**), GAP43 (violet; **A3** and **B3**), and DAPI (blue; **A4** and **B4**), as well as merged images (**A5** and **B5**) at the lesion site. Images of the 3-week EM group are shown in the left row (**A1–5**), and those of the 3-week NEM group are shown in the right row (**B1–5**). Arrowheads indicate cells positive for both tomato lectin and MMP2. Arrows indicate GAP43-structures running through the cavity-free area. Scale bars: 50 μm.

A limitation of this study is that it is based on immunohistological evaluation at the lesion site and not a molecular assay. In addition, the effect of exercise therapy on the formation of CSPGs and glial scars was not evaluated. Furthermore, the cavity formation due to neuroinflammation was not evaluated in the lesion site. The cavities are surrounded by reactive astrogliosis (Kwiecien et al., 2021). Double immuno-staining for CS-56, a pan marker of CSPGs, and GFAP, a marker for reactive astrocytes, would be necessary for further experiment to identify cavities and voids in the damaged area (Li, et al. 2020). Further additional studies are also needed to validate the molecular mechanisms of neuroinflammation and the histological changes in the lumbar region to confirm the efficacy of early mobilization.

5. Conclusion

Early mobilization of rats with spinal cord injury led to a decrease in the number of M1 microglia/macrophages and an increase in the number of M2 microglia expressing MMP2 at the acute lesion site. These changes might contribute to the recovery of hindlimb motor function.

Ethics statement

This study was carried out in accordance with the recommendations of The Yokohama City University Committee for Animal Research. The protocol was approved by the Yokohama City University Committee for Animal Research. All procedures were performed according to the standards established by the NIH Guide for the Care and Use of Laboratory Animals and the Policies on the Use of Animals and Humans in Research. All efforts were made to minimize the number of animals used and their suffering.

CRediT authorship contribution statement

Please indicate the specific contributions made by each author (list the authors' initials followed by their surnames). The name of each author must appear at least once in each of the three categories below.

Category 1.

Conception and design of study: K.A. Asano, K.F. Funakoshi, T.N. Nakamura;.

Acquisition of data: K.A. Asano;.

Analysis and/or interpretation of data: K.A. Asano, K.F. Funakoshi.

Category 2.

Drafting the manuscript: K.A. Asano, K.F. Funakoshi;.

revising the manuscript critically for important intellectual content: K.A. Asano, K.F. Funakoshi, T.N. Nakamura.

Category 3.

Approval of the version of the manuscript to be published (the names of all authors must be listed): K.A. Asano, K.F. Funakoshi, T.N. Nakamura.

Acknowledgements

All persons who have made substantial contributions to the work reported in the manuscript (e.g., technical help, writing and editing assistance, general support), but who do not meet the criteria for authorship, are named in the Acknowledgements and have given us their written permission to be named. If we have not included an Acknowledgements, then that indicates that we have not received substantial contributions from non-authors.

Acknowledgements

We are grateful to Dr. A Takeda, Y Noishiki and K Imura for specialized advice, Dr. M Takiguchi for surgical procedure advice, and Mrs. M Kobayashi and Dr. Y Atobe for experimental technical help and for experimental technical support. This research was not supported by a specific grant from funding agencies in the public, commercial, or not-for-profit sectors.

Funding

This research did not receive any specific grant from funding agencies in the public, commercial, or not-for-profit sectors.

Declaration of Interest

None.

Appendix A. Supporting information

Supplementary data associated with this article can be found in the online version at doi:10.1016/j.ibneur.2022.04.002.

References

Adams, K.L., Gallo, V., 2018. The diversity and disparity of the glial scar. Nat Neurosci. 21 (1), 9–15. https://doi.org/10.1038/s41593-017-0033-9. . Epub 2017 Dec 21. PMID: 29269757; PMCID: PMC5937232.

Alizadeh, A., Dyck, S.M., Kataria, H., Shahriary, G.M., Nguyen, D.H., Santhosh, K.T., Karimi-Abdolrezaee, S., 2017. Neuregulin-1 positively modulates glial response and improves neurological recovery following traumatic spinal cord injury. Glia 65 (7), 1152–1175, 10.1002/glia.23150. Epub 2017 Apr 29. PMID: 28456012.

AVERT Trial Collaboration group.Efficacy and safety of very early mobilisation within 24h of stroke onset (AVERT): a randomised controlled trial. Lancet. 2015 Jul 4;386 (9988):46–55. doi: 10.1016/S0140-6736(15)60690-0. Epub 2015 Apr 16. Erratum in: Lancet. 2015 Jul 4;386(9988):30. Erratum in: Lancet. 2017 May 13;389(10082): 1884. PMID: 25892679.

Basso, D.M., Beattie, M.S., Bresnahan, J.C., 1995. A sensitive and reliable locomotor rating scale for open field testing in rats. In: J. Neurotrauma, 12, pp. 1–21, 10.1089/neu.1995.12.1. PMID: 7783230.

Bellver-Landete, V., Bretheau, F., Mailhot, B., Vallières, N., Lessard, M., Janelle, M.E., Vernoux, N., Tremblay, M.È., Fuehrmann, T., Shoichet, M.S., Lacroix, S., 2019. Microglia are an essential component of the neuroprotective scar that forms after spinal cord injury. Nat. Commun. 10 (1), 518, 10.1038/s41467-019-08446-0. PMID: 30705270; PMCID: PMC6355913.

Brown, A.K., Woller, S.A., Moreno, G., Grau, J.W., Hook, M.A., 2011. Exercise therapy and recovery after SCI: evidence that shows early intervention improves recovery of function. Spinal Cord 49 (5), 623–628, 10.1038/sc.2010.167. Epub 2011 Jan 18. PMID: 21242998; PMCID: PMC3230555.

Chhaya, S.J., Quiros-Molina, D., Tamashiro-Orrego, A.D., Houlé, J.D., Detloff, M.R., 2019. Exercise-induced changes to the macrophage response in the dorsal root ganglia prevent neuropathic pain after spinal cord injury. J. Neurotrauma 36 (6), 877–890. https://doi.org/10.1089/neu.2018.5819. Epub 2018 Oct 18. PMID: 30152715; PMCID: PMC6484359.

Chiu, C.W., Huang, W.H., Kuo, H.S., Tsai, M.J., Chen, C.J., Lee, M.J., Cheng, H., 2018. Local inhibition of matrix metalloproteinases reduced M2 macrophage activity and impeded recovery in spinal cord transected rats after treatment with fibroblast growth factor-1 and nerve grafts. Neural Regen. Res. 13 (8), 1447–1454, 10.4103/1673-5374.235302. PMID: 30106058; PMCID: PMC6108206.

Cunha C., Gomes C., Vaz AR, Brites D. Exploring New Inflammatory Biomarkers and Pathways during LPS-Induced M1 Polarization. Mediators Inflamm. 2016;2016: 6986175. doi: 10.1155/2016/6986175. Epub 2016 Dec 21. PMID: 28096568; PMCID: PMC5209629.

Duchossoy, Y., Horvat, J.C., Stettler, O., 2001. MMP-related gelatinase activity is strongly induced in scar tissue of injured adult spinal cord and forms pathways for ingrowing neurites. Mol. Cell Neurosci. 17 (6), 945–956, 10.1006/mcne.2001.0986. PMID: 11414785.

Dugan, E.A., Jergova, S., Sagen, J., 2020. Mutually beneficial effects of intensive exercise and GABAergic neural progenitor cell transplants in reducing neuropathic pain and spinal pathology in rats with spinal cord injury. Exp. Neurol. 327, 113208 https://doi.org/10.1016/j.expneurol.2020.113208. Epub 2020 Jan 18. PMID: 31962127.

Dyck, S.M., Karimi-Abdolrezaee, S., 2015. Chondroitin sulfate proteoglycans: Key modulators in the developing and pathologic central nervous system. Exp. Neurol. 269, 169–187. https://doi.org/10.1016/j.expneurol.2015.04.006. Epub 2015 Apr 18. PMID: 25900055.

Goussev, S., Hsu, J.Y., Lin, Y., Tjoa, T., Maida, N., Werb, Z., Noble-Haeusslein, L.J., 2003. Differential temporal expression of matrix metalloproteinases after spinal cord injury: relationship to revascularization and wound healing. J. Neurosurg. 99 (2 Suppl), 188–197. https://doi.org/10.3171/spi.2003.99.2.0188. PMID: 12956462; PMCID: PMC2792200.

Hsu, J.Y., Bourguignon, L.Y., Adams, C.M., Peyrollier, K., Zhang, H., Fandel, T., Cun, C. L., Werb, Z., Noble-Haeusslein, LJ, 2008. Matrix metalloproteinase-9 facilitates glial scar formation in the injured spinal cord. J Neurosci. 28 (50), 13467–13477. https://doi.org/10.1523/JNEUROSCI.2287-08.2008. PMID: 19074020; PMCID: PMC2712293.

Hsu, J.Y., McKeon, R., Goussev, S., Werb, Z., Lee, J.U., Trivedi, A., Noble-Haeusslein, L. J., 2006. Matrix metalloproteinase-2 facilitates wound healing events that promote functional recovery after spinal cord injury. J. Neurosci. 26 (39), 9841–9850. https://doi.org/10.1523/JNEUROSCI.1993-06.2006. MID: 17005848; PMCID: PMC2659718.

Jeong, J.H., Lee, Y.R., Park, H.G., Lee, W.L., 2015. The effects of either resveratrol or exercise on macrophage infiltration and switching from M1 to M2 in high fat diet mice. J. Exerc. Nutrition Biochem. 19 (2), 65–72. https://doi.org/10.5717/jenb.2015.15060203. Epub 2015 Jun 30. PMID: 26244124; PMCID: PMC4523807.

Kwiecien, J.M., Dąbrowski, W., Yaron, J.R., Zhang, L., Delaney, K.H., Lucas, A.R., 2021. The role of astrogliosis in formation of the syrinx in spinal cord injury. Curr. Neuropharmacol. 19 (2), 294–303. https://doi.org/10.2174/1570159×18666200720225222. PMID: 32691715; PMCID: PMC8033977.

Ledeboer, A., Brevé, J.J., Poole, S., Tilders, F.J., Van, Dam, A.M., 2000. Interleukin-10, interleukin-4, and transforming growth factor-beta differentially regulate lipopolysaccharide-induced production of pro-inflammatory cytokines and nitric oxide in co-cultures of rat astroglial and microglial cells. Glia 30 (2), 134–142, 10.1002/(sici)1098-1136(200004)30:2<134::aid-glia3>3.0.co;2-3. PMID: 10719355.

Li, Y., He, X., Kawaguchi, R., Zhang, Y., Wang, Q., Monavarfeshani, A., Yang, Z., Chen, B., Shi, Z., Meng, H., Zhou, S., Zhu, J., Jacobi, A., Swarup, V., Popovich, P.G., Geschwind, D.H., He, Z., 2020. Microglia-organized scar-free spinal cord repair in neonatal mice. Nature 587 (7835), 613–618. https://doi.org/10.1038/s41586-020-2795-6. Epub 2020 Oct 7. PMID: 33029008; PMCID: PMC7704837.

Lu, P., Wang, Y., Graham, L., McHale, K., Gao, M., Wu, D., Brock, J., Blesch, A., Rosenzweig, E.S., Havton, L.A., Zheng, B., Conner, J.M., Marsala, M., Tuszynski, M. H., 2012. Long-distance growth and connectivity of neural stem cells after severe spinal cord injury. Cell 150 (6), 1264–1273. https://doi.org/10.1016/j.cell.2012.08.020. PMID: 22980985; PMCID: PMC3445432.

Neefkes-Zonneveld, C.R., Bakkum, A.J., Bishop, N.C., van Tulder, M.W., Janssen, T.W., 2015. Effect of long-term physical activity and acute exercise on markers of systemic inflammation in persons with chronic spinal cord injury: a systematic review. Arch. Phys. Med. Rehabil. 96 (1), 30–42. https://doi.org/10.1016/j.apmr.2014.07.006. Epub 2014 Jul 24. PMID: 25064781.

Nishihara, T., Tanaka, J., Sekiya, K., Nishikawa, Y., Abe, N., Hamada, T., Kitamura, S., Ikemune, K., Ochi, S., Choudhury, M.E., Yano, H., Yorozuya, T., 2020. Chronic constriction injury of the sciatic nerve in rats causes different activation modes of microglia between the anterior and posterior horns of the spinal cord. Neurochem. Int. 134, 104672 https://doi.org/10.1016/j.neuint.2020.104672. Epub 2020 Jan 9. PMID: 31926989.

Rolls, A., Shechter, R., London, A., Segev, Y., Jacob-Hirsch, J., Amariglio, N., Rechavi, G., Schwartz, M., 2008. Two faces of chondroitin sulfate proteoglycan in spinal cord repair: a role in microglia/macrophage activation. PLoS Med. 5 (8), e171 https://doi.org/10.1371/journal.pmed.0050171. PMID: 18715114; PMCID: PMC2517615.

Sharif-Alhoseini, M., Khormali, M., Rezaei, M., Safdarian, M., Hajighadery, A., Khalatbari, M.M., Safdarian, M., Meknatkhah, S., Rezvan, M., Chalangari, M., Derakhshan, P., Rahimi-Movaghar, V., 2017. Animal models of spinal cord injury: a systematic review. Spinal Cord 55 (8), 714–721. https://doi.org/10.1038/sc.2016.187. Epub 2017 Jan 24. PMID: 28117332.

Shinozaki, M., Iwanami, A., Fujiyoshi, K., Tashiro, S., Kitamura, K., Shibata, S., Fujita, H., Nakamura, M., Okano, H., 2016. Combined treatment with chondroitinase ABC and treadmill rehabilitation for chronic severe spinal cord injury in adult rats. Neurosci. Res. 113, 37–47. https://doi.org/10.1016/j.neures.2016.07.005. Epub 2016 Aug 4. PMID: 27497528.

Tillakaratne, N.J., Guu, J.J., de Leon, R.D., Bigbee, A.J., London, N.J., Zhong, H., Ziegler, M.D., Joynes, R.L., Roy, R.R., Edgerton, V.R., 2010. Functional recovery of stepping in rats after a complete neonatal spinal cord transection is not due to regrowth across the lesion site. Neuroscience 166 (1), 23–33. https://doi.org/10.1016/j.neuroscience.2009.12.010. Epub 2009 Dec 17. PMID: 20006680; PMCID: PMC2820384.

Trivedi, A., Noble-Haeusslein, L.J., Levine, J.M., Santucci, A.D., Reeves, T.M., Phillips, L. L., 2019. Matrix metalloproteinase signals following neurotrauma are right on cue. Cell. Mol. Life Sci. 76 (16), 3141–3156. https://doi.org/10.1007/s00018-019-03176-4. Epub 2019 Jun 6. PMID: 31168660.

Trivedi, A., Zhang, H., Ekeledo, A., Lee, S., Werb, Z., Plant, G.W., Noble-Haeusslein, L.J., 2016. Deficiency in matrix metalloproteinase-2 results in long-term vascular instability and regression in the injured mouse spinal cord. Exp. Neurol. 284 (Pt A), 50–62. https://doi.org/10.1016/j.expneurol.2016.07.018. Epub 2016 Jul 25. PMID: 27468657; PMCID: PMC5035216.

Venkatesh, K., Ghosh, S.K., Mullick, M., Manivasagam, G., Sen, D., 2019. Spinal cord injury: pathophysiology, treatment strategies, associated challenges, and future implications. Cell Tissue Res. 377 (2), 125–151. https://doi.org/10.1007/s00441-019-03039-1. Epub 2019 May 7. PMID: 31065801.

Xu, F., Huang, J., He, Z., Chen, J., Tang, X., Song, Z., Guo, Q., Huang, C., 2016. Microglial polarization dynamics in dorsal spinal cord in the early stages following chronic sciatic nerve damage. Neurosci. Lett. 617, 6–13. https://doi.org/10.1016/j.neulet.2016.01.038. Epub 2016 Jan 26. PMID: 26820376.

Zhang, Y., Liu, Z., Zhang, W., Wu, Q., Zhang, Y., Liu, Y., Guan, Y., Chen, X., 2019. Melatonin improves functional recovery in female rats after acute spinal cord injury by modulating polarization of spinal microglial/macrophages. J. Neurosci. Res. 97 (7), 733–743. https://doi.org/10.1002/jnr.24409. Epub 2019 Apr 22. PMID: 31006904.

Zhou, X., Wahane, S., Friedl, M.S., Kluge, M., Friedel, C.C., Avrampou, K., Zachariou, V., Guo, L., Zhang, B., He, X., Friedel, R.H., Zou, H., 2020. Microglia and macrophages promote corralling, wound compaction and recovery after spinal cord injury via Plexin-B2. Nat. Neurosci. 23 (3), 337–350. https://doi.org/10.1038/s41593-020-0597-7. PMID: 32112058; PMCID: PMC7412870.